Earth Syst. Dynam. Discuss., https://doi.org/10.5194/esd-2017-92
Manuscript under review for journal Earth Syst. Dynam.
Discussion started: 1 November 2017

Earth System Dynamics
Discussions
Open Access
EGU

Assessing Carbon Dioxide Removal Through Global and Regional Ocean Alkalization under High and Low Emission Pathways.

Andrew Lenton [1,2], Richard J. Matear [1], David P. Keller [3], Vivian Scott[4] and Naomi E. Vaughan[5]

[1] CSIRO Oceans and Atmosphere, Hobart Australia
[2] Antarctic Climate and Ecosystems Co-operative Research Centre, Hobart, Australia
[3] GEOMAR Helmholtz Centre for Ocean Research Kiel, Germany
[4] School of Geosciences, University of Edinburgh, Edinburgh, United Kingdom
[5]Tyndall Centre for Climate Change Research, School of Environmental Sciences, University of East Anglia, Norwich, UK.

1. Abstract

Atmospheric CO_2 levels continue to rise, increasing the risk of severe impacts on the Earth system, and on the ecosystem services that it provides. Artificial Ocean Alkalization (AOA) is capable of reducing atmospheric CO_2 concentrations, surface warming and addressing ocean acidification. Here we simulate global and regional responses to alkalinity addition (0.25 PmolAlk/year) using the CSIRO-Mk3L-COAL Earth System Model in the period 2020-2100, under high (RCP8.5) and low (RCP2.6) emissions. While regionally there are large changes associated with locations of AOA, globally we see only a very weak dependence on where and when AOA is applied. We see that under RCP2.6, while the carbon uptake associated with AOA is only ~60% of the total under RCP8.5, the relative changes in temperature are larger, as are the changes in pH (1.4x) and aragonite saturation (1.7x). The results of this modelling study are significant as they demonstrate that AOA is more effective under lower emissions, and the higher the emissions the more AOA required to achieve the same reduction in global warming and ocean acidification. Finally, our simulations show AOA in the period 2020-2100 is capable of offsetting global warming and ameliorating ocean acidification increases due to low emissions, but regionally the response is more variable.

Earth Syst. Dynam. Discuss., https://doi.org/10.5194/esd-2017-92
Manuscript under review for journal Earth Syst. Dynam.
Discussion started: 1 November 2017

1. Introduction

Atmospheric carbon dioxide (CO_2) levels continue to rise primarily as a result of human activities. Recent studies have suggested that even deep cuts in emissions may not be sufficient to avoid severe impacts on the Earth system, and the ecosystem services that it provides (Gasser et al., 2015). Recent international negotiations (UNFCCC, 2015) agreed to limit global warming to well below 2°. The application of Carbon Dioxide Removal (CDR), sometimes referred to as "Negative Emissions", appears to be required to achieve this goal, as emission reductions alone are likely to be insufficient (Rogelj et al., 2016). In this context, there is an urgent need to assess how Carbon Dioxide Removal (CDR) could help either mitigate climate change or even reverse it, and to understand the potential risks and benefits of different options.

While warming represents a major imminent global threat, including through coral bleaching which is already significantly impacting the natural environment (Hughes et al., 2017) ocean acidification poses an additional and equally significant threat to the marine environment. Ocean acidification occurs as CO_2 taken up by the ocean reacts with the seawater to reduce the carbonate ion concentration and decrease the pH. Annually the oceans take up about 28% of anthropogenic CO_2 emitted (Le Quéré et al., 2015).

Ocean acidification is the unavoidable consequence of rising atmospheric CO_2 levels and will impact the entire marine ecosystem - from plankton at the base, to fish at the top. Potential impacts include changes to calcification, fecundity, organism growth and physiology, species composition and distributions, food web structure and nutrient availability (Doney et al., 2012;Dore et al., 2009;Fabry et al., 2008;Iglesias-Rodriguez et al., 2008;Munday et al., 2010;Munday et al., 2009). Within this century, the impacts of ocean acidification will increase in proportion to emissions (Gattuso et al., 2015). Furthermore, these changes will be long lasting, persisting for centuries or longer even if emissions were halted (Frolicher and Joos, 2010).

To date many different CDR techniques have been proposed both on the land and in the ocean (Royal Society, 2009;National Research Council, 2015). Their primary purpose is to reduce atmospheric CO_2 levels; and most CDR methods will ameliorate the impacts of ocean acidification, although some proposed techniques such as ocean pipes (Lovelock and Rapley,

2007) and micro-nutrient addition (Keller et al., 2014) may actually lead to an acceleration of ocean acidification in surface waters.

Artificial Ocean Alkalization (AOA) through altering the chemistry of seawater both enhances ocean carbon uptake, thereby reducing atmospheric CO_2, while at the same time directly reversing ocean acidification. AOA can be thought of as a massive acceleration of the natural processes of chemical weathering of minerals that may have played a role in modulating the climate on geological timescales (Zeebe, 2012;Colbourn et al., 2015). Alkalinity changes may also have played an important role in controlling glacial-interglacial cycles of atmospheric CO_2 e.g. Sigman and Boyle (2000).

Specifically, as alkalinity enters the ocean the pH increases leading to elevated carbonate ion concentration, reduction in hydrogen ion concentration and decrease in the concentration of aqueous CO_2 (or pCO_2). This in turn enhances the disequilibrium of CO_2 between the ocean and atmosphere (or $\Delta pCO_2 = pCO_2^{ocean} - pCO_2^{atmosphere}$) leading to increased ocean carbon uptake, and reduction in atmospheric CO_2 concentration. These increases in pH and carbonate ion concentration reverse the ocean acidification due to uptake of anthropogenic CO_2.

Kheshgi (1995) first proposed AOA as a method of CDR. Renforth and Henderson (2017) review the early experimental, engineering and modelling work undertaken to investigate AOA. From the observational perspective we draw particular attention to the experimental work of Albright et al. (2016) which provided an in situ demonstration of localised AOA to offset the observed changes in ocean acidification on the Great Barrier Reef that have occurred since the pre-industrial period.

Several modelling studies have explored the impacts of AOA both on carbon sequestration and ocean acidification. Using ocean only biogeochemical models Kohler et al. (2013) explored AOA via olivine addition. Olivine, in addition to increasing alkalinity also adds iron and silicic acid, both of which can enhance ocean productivity (Jickells et al., 2005;Ragueneau et al., 2000). Kohler et al. (2013) estimated the response of atmospheric CO_2 levels and pH to different levels of olivine addition over the period 2000-2010, and later this was extended to 2100 by Hauck et al. (2016). These studies demonstrate a global impact, that appeared to scale with the amount of olivine added. Importantly, Kohler et al. (2013)

showed that the global effect of alkalinity added along shipping routes (as an analogue for practical implementation) was not significantly different from that of alkalinity added in a highly idealized uniform manner.

Ilyina et al. (2013) explored the potential of AOA to mitigate rising atmospheric CO_2 levels and ocean acidification in ocean-only biogeochemical simulations, and showed that AOA has the potential to ameliorate future changes due to high emissions. They did not limit the amount of AOA, as their goal was to offset the projected future changes; and showed that the amount of AOA required to do this would drive the carbonate system to levels well above pre-industrial levels. Ilyina et al. (2013) also conclude that local AOA could potentially be used to offset the impact of ocean acidification, with enhanced CO_2 uptake being only a side benefit. This regional approach was explored further by Feng et al. (2016) who suggested that local AOA in the tropical ocean, in areas of high coral calcification, has the potential to offset the impact of future rising atmospheric CO_2 levels under a high emissions scenario (RCP8.5). This study also revealed strong regional sensitivities in the response of ocean acidification related to the locations in which it was applied.

To date several studies estimate the response of the Earth system to AOA. Gonzalez and Ilyina (2016) used an Earth System Model (ESM) to estimate the AOA required to reduce atmospheric concentrations from high emissions scenario (RCP8.5) to the medium emissions scenario (RCP4.5). They estimated that to mitigate the associated 1.5K warming difference, via reducing atmospheric CO_2 concentrations by ~400 ppm, would require an addition of 114 Pmol of alkalinity (between 2018-2100), and would come at the cost of very large (unprecedented) changes in ocean chemistry.

Keller et al. (2014) used an Earth System Model of Intermediate Complexity (EMIC) to explore the impact of AOA over the period 2020-2100, to a globally uniform addition of alkalinity (0.25 PmolALK/yr), an amount based on the estimated carrying capacity of global shipping following Kohler et al. (2013). Keller et al. (2014) showed that AOA led to reduction in atmospheric CO_2 of 166 PgC or ~78ppm, a net cooling of 0.26K and a global increase in ocean pH of 0.06 in the period 2020-2100.

To date not all modelling studies have been emissions driven, and this is important as potential climate and carbon cycle feedbacks may not have been accounted for. Capturing

these feedbacks is critical as they have the potential to be very large (Jones et al., 2016). Further, no studies have explored the impact of AOA under low emissions scenarios such as RCP2.6. This is important because scenarios that limit warming to 2° or less, currently utilize considerable land based CDR via afforestation and/or Bio-Energy with Carbon Capture and Storage (BECCS) the feasibility of which are increasingly questioned due in part to limited land (Smith et al., 2016), whereas the potential CDR capacity of the oceans is orders of magnitude greater (Scott et al., 2015).

In this work, using a fully coupled Earth System Model (CSIRO-Mk3L-COAL), which includes climate and carbon feedbacks, we investigate the impact of AOA on ocean acidification, land and ocean carbon uptake and warming. Specifically, the question this study tackles is: What is the impact of global and regional AOA on the Earth System, and how efficient it is at mitigating global warming and ocean acidification under high and low emissions trajectories?

2. Methods

2.1 Model Description

The model simulations were performed using the CSIRO-Mk3L-COAL (Carbon Ocean, Atmosphere, Land) Earth System Model which includes climate-carbon interactions and feedbacks. (Matear and Lenton, 2014;Zhang et al., 2014a). The ocean component of the Earth System Model has a resolution of 2.8° by 1.6° with 21 vertical levels. The ocean biogeochemistry is based on (Lenton and Matear, 2007;Matear and Hirst, 2003) simulating the distributions of phosphate, oxygen, dissolved inorganic carbon and alkalinity in the ocean. The model simulates particulate inorganic carbon (PIC) production as function of particulate organic carbon (POC) production via the rain ratio (9%) following (Yamanaka and Tajika, 1996). This ocean biogeochemical model was shown to simulate the observed distributions of total carbon and alkalinity in the ocean (Matear and Lenton, 2014) and phosphate (Duteil et al., 2012).

The atmosphere resolution is 5.6° x 3.2° with 18 vertical layers. The land surface scheme uses CABLE (Best et al., 2015) coupled to CASA-CNP (Wang et al., 2010;Mao et al., 2011) which simulates biogeochemical cycles of carbon, nitrogen and phosphorus in plants and soils. The response of the land carbon cycle was shown to realistically simulate the observed biogeochemical fluxes and pools on the land surface (Wang et al., 2010).

To quantify the changes in ocean acidification we calculate pH changes on the total scale following the recommendation of Riebesell et al. (2010). To calculate the changes of carbonate saturation state we use the equation of Mucci (1983).

2.2 Model Experimental Design

Our ESM was spun-up under a preindustrial atmospheric CO_2 concentration of 284.7 ppm, until the simulated climate was stable (> 2000 years) (Phipps et al., 2012). From the spun-up initial climate state, the historical simulation (1850 - 2005) was performed using the historical atmospheric CO_2 concentrations as prescribed by the CMIP5 simulation protocol (Taylor et al., 2012).

Following the historical concentration pathway from 2006, two different future projections to 2100 were made using the atmospheric CO_2 emissions corresponding to Representative Concentration Pathways of low emissions (RCP2.6) and high emissions (RCP8.5 or 'business as usual') (Taylor et al., 2012). All simulations include the forcing due to non-CO_2 greenhouse gas concentrations (Taylor et al., 2012). We define RCP8.5 and RCP2.6 as our control cases for the corresponding experiments below.

In the period 2020-2100 we undertook a number of AOA experiments using a fixed quantity of 0.25 Pmol/yr of alkalinity, the same amount used by Keller et al. (2014). Consistent with this study we applied AOA in the surface ocean all year-round in ice-free regions, set to be between 60°S and 70°N. For each of the two emissions scenarios, we considered four different regional applications of AOA, shown in Figure 1. These are: (i) AOA globally (AOA_G) between 60S and 70N; (ii) the higher latitudes comprising the subpolar northern hemisphere oceans (40N -70N) and the (ice-free) Southern Ocean (40S-60S) (AOA_SP); (iii) the subtropical oceans (15-40N and 15S and 40S; AOA_ST); and (iv) in the equatorial regions (15N-15S; AOA_T). In this study, we only look at the response of the Earth system to alkalinity injection. We do not consider the biogeochemical response to other minerals and elements associated with the proposed sourcing of alkalinity from the application of finely ground ultra-mafic rocks such as olivine and fosterite, nor dissolution processes required to increase alkalinity e.g. Montserrat et al. (2017).

3. Results and Discussion

To aid in presenting our results and to compare these with previous studies we first discuss the carbon cycle, global surface warming (2m surface air temperature), and response and ocean acidification response to the 4 different AOA experiments under the high (RCP8.5) and low (RCP2.6) emissions scenarios. We then look at the regional behaviour of the simulations in the different AOA experiments.

3.1 Global Response

For each emission scenario, we simulated 4 different AOA experiments, which all had the same 0.25 Pmol/yr of alkalinity added. As anticipated by 2100, AOA increased the global mean surface ocean alkalinity relative to the corresponding scenario control case, with the magnitude of the increase in alkalinity being dependent on where it was added (Table 1). Polar addition (AOA_SP) led to the smallest net increase in surface alkalinity, while tropical addition (AOA_T) produced the greatest increase. As expected, the global mean changes in surface alkalinity between emissions scenarios are very small (less than 3 μmol/kg difference). The slightly greater increase in surface values in alkalinity under RCP8.5 likely reflects enhanced ocean stratification under higher emissions (Yool et al., 2015).

	RCP8.5	RCP2.6
AOA_G -RCP	108.3	105.1
AOA_SP-RCP	79.7	74.4
AOA_ST-RCP	115.1	112.9
AOA_T-RCP	129.8	127.1

Table 1 For the two RCP scenarios the relative increase in ocean surface alkalinity (μmol/kg) between each AOA experiment and control experiment in 2100.

3.1.1 Carbon Cycle

The large atmospheric CO_2 concentration at the end of the century under RCP8.5 reflects the large increase in emissions projected (under RCP8.5), while under RCP2.6 a similar atmospheric concentration of CO_2 is seen 2100 as at the beginning of the simulation (2020) (Figure2a). We note that atmospheric CO_2 levels in our CSIRO-MK3L-COAL for the control cases are greater than for their respective concentration driven RCPs due to nutrient limitation in the land, leading to reduced carbon uptake (Zhang et al., 2014a) .

236
237 Under all emissions scenarios and experiments AOA leads to reduced atmospheric CO_2
238 levels (Figure 2a). Under RCP8.5, AOA reduces atmospheric concentration by 82-86 ppm,
239 this represents ~16% decrease in atmospheric concentration (525 ppm increase over the
240 period 2020-2100). In contrast to RCP8.5, AOA under RCP2.6 leads to a smaller reduction in
241 atmospheric concentration (53-58 ppm). Figure 2a shows that by the of the century AOA
242 more than compensates for the projected increase in atmospheric CO_2 due to RCP2.6.
243
244 Over the 2020-2100 period, the reduction in atmospheric CO_2 levels associated with AOA is
245 primarily due to increased ocean carbon uptake, offset by small decreases in the land surface
246 carbon uptake (Table 2). In the ocean, RCP8.5 has much greater net uptake than RCP2.6,
247 about 1.5 times more, due to the larger (and growing) disequilibrium between the atmosphere
248 and ocean.
249
250 In the ocean, the relative increase in carbon uptake in response to AOA is primarily abiotic in
251 nature. Consistent with Keller et al. (2014) and Hauck et al. (2016) the simulated changes in
252 ocean export production were very small (~0.2 PgC) under RCP8.5. While under RCP2.6 it
253 was slightly larger at 1.2 PgC, but still less than 1% percent of the total ocean increase
254 simulated under AOA. In contrast, the relative decreases in land carbon uptake were biotic in
255 nature. The simulated cooling over land drove a reduction in net primary production that
256 more than offset the decrease in carbon flux due in heterotrophic respiration. On the land, the
257 RCP8.5 simulated a smaller reduction in carbon uptake than RCP2.6, potentially due to a
258 smaller relative cooling (Table 3).
259
260 For both emissions scenarios, the 4 AOA experiments all produced similar reductions in
261 atmospheric CO_2 concentrations (Figure 2) with less than a 5% difference in the total land
262 and ocean carbon uptake. The global changes in land and ocean carbon uptake do not appear
263 to be very sensitive to where we add the alkalinity to the surface ocean. This is consistent
264 with Kohler et al. (2013) who saw little difference in adding olivine along existing shipping
265 tracks, versus uniformly adding it to the surface ocean. It is also consistent with regional
266 addition studies Ilyina et al. (2013) and Feng et al. (2016) who demonstrated a global impact.
267
268 Our simulated total increased carbon uptake under AOA_G with RCP8.5 (179 PgC) is
269 comparable to the 166 PgC reported by (Keller et al., 2014). Their cumulative increase in

Earth Syst. Dynam. Discuss., https://doi.org/10.5194/esd-2017-92
Manuscript under review for journal Earth Syst. Dynam.
Discussion started: 1 November 2017

ocean carbon uptake by 2100 of 181 PgC was in very good agreement with our value of 184 PgC. However, they simulated a reduction in land uptake nearly twice the -5.8 PgC reduction in our AOA_G simulation. These differences may reflect both the sensitivity of the simulated climate feedbacks, and differences in land surface models.

	Total RCP8.5	Ocean RCP8.5	Land RCP8.5	Total RCP 2.6	Ocean RCP 2.6	Land RCP 2.6
AOA_G-RCP	178.6	184.4	-5.8	121.1	143.1	-22.1
AOA_SP-RCP	183.3	188.1	-4.8	122.1	145.2	-24.1
AOA_ST-RCP	180.7	185.1	-4.4	122.0	143.1	-21.2
AOA_T-RCP	174.5	177.2	-2.7	116.0	139.2	-23.1

Table 2 The total integrated additional carbon uptake (in PgC) in the period 2020-2100 in different experiment and emissions scenarios, negative denotes enhanced uptake.

3.1.2 Surface Air Temperature

In the control simulations, the global mean surface air temperature (SAT; 2m) increased in the period 2020-2100 with RCP2.6 simulating a net warming of 0.4±0.1K while RCP8.5 warmed by 2.7±0.1K (2081-2100). All AOA experiments simulated a reduction in global mean SAT relative to their corresponding control simulation (Figure 2b). Within each emissions scenario the global mean SAT decline associated with AOA is always greater and more variable over the land than ocean (Table 3). While the mean cooling, in the period 2081-2100, is also greater over the land under RCP8.5 than RCP2.6, potentially reflecting feedbacks such as soil-moisture (Seneviratne et al., 2010) snow and ice cover changes. However, these changes are associated with large interannual large variability, and therefore not significantly different.

Under RCP2.6, all the AOA experiments keep warming levels much close to values in 2020 than RCP2.6 by the end of this century (2100; Figure 2b). In contrast, under the RCP8.5 scenario, none of the AOA experiments have a significant impact on the projected warming

by the end of this century (less than 10%) reflecting the large warming anticipated under high emissions (Rogelj et al., 2012).

	Total RCP8.5	Ocean RCP8.5	Land RCP8.5	Total RCP 2.6	Ocean RCP 2.6	Land RCP 2.6
AOA_G-RCP	-0.16±0.08	-0.14±0.07	-0.22±0.15	-0.25±0.08	-0.19±0.05	-0.39±0.22
AOA_SP-RCP	-0.13±0.10	-0.11±0.07	-0.18±0.20	-0.23±0.08	-0.18±0.05	-0.35±0.22
AOA_ST-RCP	-0.08±0.05	-0.06+0.03	-0.13±0.14	-0.20±0.09	-0.15±0.06	-0.30±0.20
AOA_T-RCP	-0.14±0.06	-0.12±0.05	-0.19±0.11	-0.16±0.06	-0.13±0.05	-0.24±0.16

Table 3 The differences in global mean surface air temperature and their standard deviations (1-σ) (K; SAT; 2m) for 2090 (in the period 2081-2100) for different AOA experiments and emissions scenarios relative to the emissions scenarios with no AOA.

Within each of the scenarios, there is some variability in the magnitude of the cooling within the 4 different AOA experiments, however, these differences are smaller than the interannual variability over the last 2 decades of the simulations. Therefore, it appears that the global mean SAT decline with AOA is not very sensitive to where the alkalinity is added under either emission scenario.

The global mean cooling associated with AOA_G under RCP8.5 (-0.16±0.08K; 2081:2100) is close to the mean surface air temperature decrease of -0.26K reported by (Keller et al., 2014) for the same levels of AOA. These differences may reflect the simplified atmospheric representation of the UVIC Intermediate Complexity Model and different climate sensitivities.

3.1.3 Ocean Acidification

Here we quantify changes in ocean acidification in terms of pH and aragonite saturation state changes. We consider these two diagnostics because they are associated with different

biological impacts and not necessarily well correlated (Lenton et al., 2016). In the future, the global mean changes in pH and aragonite saturation state will be proportional to the emissions trajectories following Gattuso et al. (2015) with the largest changes associated with the higher emissions (RCP8.5) (Figure 2c-d). By 2100 despite a return to 2020 values of atmospheric CO_2 concentration under RCP2.6 (Figure 2), neither pH or aragonite saturation state return to 2020 values, consistent with Mathesius et al. (2015).

In the 2020-2100 period, AOA under RCP2.6 led to much larger increases in surface pH and aragonite saturation state, more than 1.3 times, and more than 1.7 times that of RCP8.5 respectively (Table 4). These changes reflect the differences in the mean state associated with high and low emissions, specifically the difference between Alkalinity and DIC. The values of DIC in the upper ocean are larger under RCP8.5 than RCP2.6, and therefore the ALK-DIC is higher. For a given addition of alkalinity, the increase in the upper ocean DIC will be greater in the high emission case than the low emission case due to the Revelle Factor (Revelle and Suess, 1957). Consequently, the difference between Alkalinity and DIC with AOA increases less in the high emission scenario than the low scenario, which translates into smaller increases in pH and aragonite saturation state in the high scenario.

While there was a significant difference in pH and aragonite saturation state changes with AOA between high and low emissions cases, the global mean changes for different AOA experiments within each scenario is quite similar (Table 4). The exception being the AOA_SP experiment, where its pH and aragonite saturation state changes are only ~75% of the change in the other AOA experiments. This reduced change in the polar region is consistent with the smaller changes in the surface ocean alkalinity values associated with AOA_SP (Table 1). These differences at higher latitudes reflect the enhanced subduction of alkalinity away from the surface ocean into the ocean interior that occurs in the high latitude oceans (Groeskamp et al., 2016).

AOA_G under RCP8.5 leads to a relative increase in pH of 0.06 which is consistent with (Keller et al., 2014), while our relative increase in aragonite saturation state (0.28) is also very close to their simulated value (0.31). To put these changes into context, the estimated decrease in pH since the preindustrial is 0.1 units (Raven et al., 2005).

Earth Syst. Dynam. Discuss., https://doi.org/10.5194/esd-2017-92
Manuscript under review for journal Earth Syst. Dynam.
Discussion started: 1 November 2017

	Aragonite RCP8.5	pH RCP8.5	Aragonite RCP2.6	pH RCP 2.6
AOA_G-RCP	0.28	0.06	0.50	0.07
AOA_SP-RCP	0.20	0.05	0.39	0.07
AOA_ST-RCP	0.30	0.06	0.54	0.08
AOA_T-RCP	0.28	0.06	0.5	0.07

Table 4 The relative differences in surface value of aragonite saturation state and pH between the AOA experiments and the high and low emissions scenarios in 2100

3.2 Regional Responses

For both RCP scenarios, there are large regional differences in the relative surface changes in alkalinity, temperature, and ocean acidification associated with the different AOA experiments. The regional nature of these changes is closely associated with where alkalinity addition is applied, and the two different emissions scenarios considered here do not differ significantly in their behaviour. This implies that any differences in stratification and overturning circulation between the two scenarios are insufficient to significantly modulate the response to AOA.

3.2.1. Surface Alkalinity

For both scenarios, the greatest surface alkalinity changes occur where the alkalinity is added (Figure 3). Spatially under either emission scenario, the relative differences in 2090 are very similar, consequently we only show the changes under RCP2.6 (Figure 3). The only significant differences occur in the Arctic, reflecting larger longer-term changes in alkalinity projected under higher emissions (Yamamoto et al., 2012).

Overall the greatest increases are seen in the tropical ocean (AOA_T) suggesting this is the most efficient region in retaining the added alkalinity in the upper ocean. This reflects the fact that subduction processes in the tropical ocean are less efficient than other regions such as the higher latitudes. In the (ice-free) subpolar oceans (AOA_SP) produced the smallest relative increase in alkalinity, and this reflects the strong and efficient surface to interior

connections occurring at higher latitudes (Groeskamp et al., 2016). The global mean relative increase associated with AOA in the subtropical gyres (AOA_ST) and globally (AOA_G) fall between the tropical and higher latitude values. In the case of AOA_ST this reflects the time-scales associated with circulation of the subtropical gyres.

The most modest relative increase in alkalinity occurs in the non-ice-free regions where alkalinity is not explicitly added. Interestingly even when alkalinity is added in the very high latitude Southern Ocean it is carried northward by the Ekman current explaining the very modest increase in the region where AOA occurs between 50S to 60S. In terms of the total alkalinity added to the surface ocean, about one-third remains in the upper 200m in 2100. Specifically, for AOA_G we see 31% remains, AOA_T and AOA_ST: 34%, while for AOA_SP: 22-24% remains, which (as anticipated) is lower than in other regions.

Spatially AOA in the higher latitude regions (AOA_SP) leads to very large relative increases in alkalinity (> 1000 μmol/kg; 2090) occurring along the northern most boundary of the Northern Subpolar Gyres, particularly the North Pacific. Clearly in this region the rate of AOA exceeds the rate of subduction allowing alkalinity to build up. Large relative increases in alkalinity also occur in the Southern Ocean under AOA_SP, particularly along Western Boundary Currents. However, in contrast to northern high latitudes the values still remain quite low suggesting that the rate of addition does not exceed the rate of subduction even under the highest emission scenario.

AOA_ST shows a large relative increase of ~300 μmol/kg (2081-2100) in the subpolar gyre regions. Overall, we find that these relative increases are quite homogenous across the entire subtropical gyres, with strong mixing with tropical waters leading to significant relative increases in tropical Atlantic, Western Pacific and Indian Oceans. Within the tropical ocean, under AOA_T the largest relative changes are found across the entire tropical Indian Ocean (~ 400 μmol/kg) with large relative increases also seen the Indonesian seas (~280 μmol/kg; 2081-2100). Away from the tropical Indian Ocean we find that relatively homogenous increases occur in the Western Pacific and the Atlantic, with much more modest relative increases in the Eastern Pacific reflecting the dominant East to West upper ocean circulation. Consistent with the response of AOA_ST, AOA_T leads to relative increases in surface alkalinity in the AOA_ST region of ~130 μmol/kg (2081-2100).

410
411 In the case of AOA_G a relatively uniform net increase in alkalinity occurs in all regions
412 with the exception of the upwelling regions such as the tropical Pacific, which showed a
413 more modest relative increase. In AOA_G there is little evidence of any of the very large
414 increases in alkalinity seen in the more regional AOA experiments. This spatial pattern of
415 relative increase is broadly consistent with the pattern of global alkalinity increase simulated
416 by Ilyina et al. (2013) and Keller et al (2014) for AOA in the (ice-free) global ocean.
417
418 *3.2.2 Changes in the interior distribution of alkalinity in the global ocean*
419
420 As only about 30% of the total AOA remains in the upper 200m, we explore the fate of this
421 alkalinity in the interior ocean in the zonal sections of alkalinity (Figure 4). As the pattern is
422 very similar, between RCP2.6 and RCP8.5 we only show RCP2.6, noting that in the North
423 Atlantic where the projected ocean stratification is stronger under higher emissions (not
424 shown) leading to slightly decreased subsurface values. This increased stratification is
425 consistent with other studies e.g. (Yool et al., 2015).
426
427 Unlike the surface plots of AOA, the relative increases in alkalinity due to AOA are very
428 similar across all experiments. This heterogeneous pattern of alkalinity increase is associated
429 with water entering the interior ocean along specific surface to interior pathways (Groeskamp
430 et al., 2016). Specifically, we see alkalinity moving into the interior ocean along the poleward
431 boundaries of the subtropical gyres, associated with the formation and subduction of mode
432 waters, and an increase in the subtropical gyres associated with large-scale downwelling, and
433 deep mixing in the North Atlantic. The changes in alkalinity are mainly found in the upper
434 ocean (<1000 m) which reflects the relatively short period of alkalinity addition. Given the
435 short period this is analogous to present-day observed distributions of anthropogenic carbon
436 (Sabine et al., 2004).
437
438 As the changes in export production are very small, the large changes in the interior alkalinity
439 concentrations primarily reflect the physical transport, rather than the sinking and
440 remineralization of calcium carbonate. Clearly other biological processes, not represented in
441 our model, have the potential to impact the surface and interior values of alkalinity (Matear
442 and Lenton, 2014). One such process is the reduction in ratio of PIC:POC under higher
443 emissions (Riebesell et al., 2000) however it has been shown that even a very large reduction

444 in PIC production (50%) would not significantly impact our results (Heinze, 2004)
445 Unfortunately, at present, the magnitude and sign of many of these other feedbacks remains
446 poorly known (Matear and Lenton, 2014) consequently quantifying their impact on our
447 results is very difficult, and beyond the scope of this study.
448
449 *3.2.3 Ocean Carbon Cycle Response*
450
451 The similarity in global ocean carbon uptake associated with all AOA experiments for a
452 given emission scenario hides the large spatial differences between simulations. Given that
453 the largest carbon cycle response occurs in the ocean (Table 2), we focus on this response for
454 RCP8.5 and RCP2.6 (Figures 5 and 6). As expected ocean carbon uptake is strongly
455 enhanced in the regions of AOA. Away from regions of AOA there is a reduction in carbon
456 uptake, associated with the weakening of the gradient in CO_2 between the atmosphere and
457 ocean due to AOA. Interestingly the largest increase spatially occurs in the Southern Ocean
458 under AOA_SP for RCP2.6, while in contrast the largest changes under RCP8.5 occurs in the
459 tropical ocean under AOA_SP. The very small changes in export production in RCP2.6 were
460 located in the Arabian Sea (not shown), and while these changes are < 1% of the total change
461 in carbon uptake, nevertheless they maybe important regionally.
462
463 *3.2.4 Temperature (SAT)*
464
465 The decrease in global mean SAT associated with all AOA experiments for a given emission
466 scenario again hides the large spatial differences between the simulations. The response of
467 surface temperature is spatially very heterogeneous (Figures 7 and 8), and while the regional
468 surface temperature changes are very similar between the two emissions scenarios. The
469 exception to this is the Arctic which did not show a consistent response across the different
470 AOA experiments. Under both emission scenarios, the largest cooling associated with AOA
471 occurs over Northern Russia and Canada, and Antarctica (greater than a -1.5K cooling) with
472 a larger cooling in these regions under RCP2.6.
473
474 In the surface ocean, AOA in the RCP2.6 scenario shows a net cooling over the ocean, with
475 the exception of the North Atlantic, east of New Zealand, and off the southern coast of
476 Alaska which show very a modest warming. A similar pattern is evident in RCP8.5 however

there is a greater cooling in the high latitudes, and less cooling in the lower latitudes than under RCP2.6.

3.2.5 Ocean Acidification Response

Globally the response of pH and aragonite saturation state associated with AOA are similar, however large spatial and regional differences are present. To aid in the interpretation of changes in aragonite saturation state, overlain on the aragonite saturation state maps (Figures 9 and 10) are the contours corresponding to the value of 3, the approximate threshold for suitable coral habitat (Hoegh-Guldberg et al., 2007). On these surface maps and subsequent section plots (Figures 13 and 14) we plot the saturation horizon i.e. the contour corresponding to the transition from chemically stable to unstable (or corrosive), i.e. aragonite saturation state is equal to 1 (Orr et al., 2005).

The largest relative changes in pH and aragonite saturation state were associated with regions of AOA, reflecting increases in the surface values of alkalinity. All simulations increase pH and aragonite saturation state in the Arctic despite no direct addition in this region, with the largest changes here associated with AOA_G and AOA_SP. Interestingly all simulations show little to no increase in the high latitude Southern Ocean, consistent with more efficient transport of the added alkalinity into the ocean interior.

The changes in pH associated with AOA experiments under RCP8.5 while spatially very different, particularly when added in the subpolar ocean, are still much less than the decreases associated with RCP8.5 with no AOA. In terms of aragonite saturation state the conditions for coral growth in the tropical ocean remain very unfavorable by the end of century (i.e. aragonite saturation state < 3) under all regional and global experiments, with the exception of AOA_T, where only a very small region in the Central Pacific Ocean exhibits suitable conditions.

Consistent with Feng et al. (2016) we find that this level of AOA under RCP8.5 is insufficient to ameliorate or significantly alter the large-scale changes in ocean acidification. More positively, at the higher latitudes the saturation horizon is moved poleward with the largest shift associated with AOA_SP, and the smallest shift at the high latitudes occurring under AOA_T. Consistent with these changes we see a deepening of the saturation horizon

511 everywhere (Figure 13), and little difference spatially between AOA experiments, consistent
512 with zonal mean changes in alkalinity for the 4 AOA experiments.
513
514 The spatial pattern of changes associated with AOA under RCP2.6 are broadly consistent
515 with those seen under higher emissions, however the magnitude of the response is much
516 larger again due to the larger differences between Alkalinity and DIC with AOA under
517 RCP2.6. In terms of aragonite saturation state, the area of tropical ocean favourable for corals
518 is considerably expanded suggesting that conditions for tropical coral growth are improved
519 under AOA. As anticipated the largest changes in the area favourable for tropical corals is
520 associated with AOA_T, closely followed by AOA_ST. As the saturation horizon does not
521 reach the surface under RCP2.6 we can only look at the changes in the interior ocean. Here
522 there is a deepening in the saturation horizon in all experiments of a very similar magnitude
523 (Figure 14), with the exception of the Arctic. Here the response of the saturation horizon is
524 more sensitive to the location of the AOA varying between ~100m under AOA_T and ~280
525 m under AOA_SP.
526
527 Spatially the large changes in ocean acidification in response to AOA under RCP2.6 more
528 than compensate for the changes in ocean chemistry due to low emissions in the period 2020-
529 2100. Globally, in the changes in the period 2020-2100 are sufficient to reversed or
530 compensate the changes since the preindustrial (1850). However spatially in some regions
531 such as equatorial upwelling, an important area of global fisheries (Chavez et al., 2003),
532 AOA in fact leads to higher values of aragonite saturation state and pH than the ocean
533 experienced in preindustrial period (Feely et al., 2009). We can only speculate on the
534 potential impact on marine biota through a reduction in aqueous CO_2 and elevated pH levels
535 in these regions. For a recent review of the potential impact of rising pH and Aragonite
536 saturation state on marine organisms we direct the reader to Renforth and Henderson (2017).
537
538 *3.2.6 Importance of Seasonality*
539
540 In this paper, while we have focused on year-round AOA, as a sensitivity experiment we also
541 explored whether AOA added in summer or winter was more efficient. To do this we focused
542 on the higher latitudes regions where the largest seasonal changes in mixing are found (de
543 Boyer Montegut et al., 2004;Trull et al., 2001). Here we tested whether AOA in either
544 summer or winter was more effective than year-round addition. To test this for RCP8.5 we

545 add alkalinity only during the summer at half of the annual rate (or 0.125PmolALK/year) in
546 the AOA_SP region.
547
548 Our results showed that the response to AOA in summer was very close to 50% of the
549 response of the year-round addition associated with AOA_SP (or 0.25PmolALK/year). This
550 suggests that the response of AOA appears invariant to when the alkalinity is added. This
551 also suggests, consistent with published studies e.g. (Keller et al., 2014;Feng et al.,
552 2016;Kohler et al., 2013) that the response of the ocean to different quantities of AOA is
553 scalable under the same emissions scenario. Whether this is true under very much larger
554 additions of alkalinity as simulated by (Gonzalez and Ilyina, 2016) is less clear.
555
556 **4. Summary and Concluding Remarks**
557
558 Integrated Assessment Modelling for the Intergovernmental Panel on Climate Change shows
559 that CO_2 removal (CDR) may be required to achieve the goal of limiting warming to well
560 below 2° (COP21) (Fuss et al., 2014). Of the many schemes that have been proposed to limit
561 warming, only Artificial Ocean Alkalization (AOA) is capable of both reducing the rate and
562 magnitude of global warming through reducing atmospheric CO_2 concentrations, while
563 simultaneously directly addressing ocean acidification. Ocean acidification, while receiving
564 often less attention, is likely to have very long lasting and damaging impacts on the entire
565 marine ecosystem, and the ecosystem services it provides.
566
567 Here, for the first time we investigate the response of a fully coupled climate ESM, i.e. that
568 accounts for climate-carbon feedbacks, under high (RCP8.5) and low (RCP2.6) emissions
569 scenarios to a fixed addition of alkalinity (0.25PmolALK/year). We explore the effect of
570 global and regional application of AOA focusing on the subpolar gyres, the subtropical gyres
571 and the tropical ocean. To assess AOA, we look at changes in surface air temperature, carbon
572 cycling and ocean acidification (aragonite saturation state and pH) in the period 2020-2100.
573
574 Consistent with other published studies we see that AOA leads to reduced atmospheric CO_2
575 concentrations, cooler global mean surface temperatures, and reduced levels of ocean
576 acidification. Globally for these metrics we observed that they do not vary significantly
577 between the various AOA experiments under each emissions scenario. This implies that at
578 this scale there is little sensitivity of the global responses to the region where AOA is applied.

We also investigate as a sensitivity experiment adding alkalinity in different seasons and see little difference in response to when AOA was undertaken.

We see under AOA that the increased carbon uptake is dominated by the ocean. Under RCP8.5 the changes due to AOA are only capable of reducing atmospheric concentrations by a maximum of 86 ppm versus the projected change of 560ppm, and as such the response of the climate system remains strongly dominated by warming. This is consistent with published studies of the response of the climate system under RCP8.5, and studies that have estimated the amount of AOA required to counteract a high emissions trajectory.

In contrast AOA under RCP2.6 while only capable of reducing atmospheric CO_2 levels by 58 ppm, is sufficient to reduce atmospheric CO_2 concentrations and warming to close to 2020 levels at the end of the century. This is significant as it suggests that in combination with rapid reduction in emissions, AOA could make an important contribution to the goal to keep global mean temperatures below 2°. However, AOA under RCP2.6 does not ameliorate spatial changes of carbon uptake associated with RCP2.6, resulting in a reduced uptake in the terrestrial biosphere and increased uptake in the ocean. This highlights that while the atmospheric CO_2 and warming may be reversible, the response of individual components of the Earth System to different CDR may not be (Lenton et al., 2017).

Interestingly despite the impact of AOA on the atmospheric CO_2 concentration under RCP2.6 being only ~60% of the value the under RCP8.5, we see much larger changes in ocean acidification associated with RCP2.6 than RCP8.5, more than 1.3 times in pH and more than 1.7 times in aragonite saturation state. This reflect the larger reductions of the difference between ALK and DIC that occurs under RCP2.6. We also see larger relative decreases in global temperature associated with RCP2.6. These results are very important as they demonstrate that that AOA is more effective under lower emissions in reducing ocean acidification and global warming.

While there is little sensitivity in the global responses to the region in which AOA is applied, spatially the largest changes in ocean acidification (and ocean carbon uptake) were seen in the regions where AOA was applied. Despite large changes regionally these cannot compensate for the large changes associated with RCP8.5. Even targeted AOA in the tropical ocean can preserve only a tiny area of the ocean conducive to healthy coral growth; and even

then the concomitant large warming is likely to be a stronger influence on coral growth than ocean chemistry (D'Olivo and McCulloch, 2017).

In contrast AOA under RCP2.6 is more than capable of ameliorating the projected ocean acidification changes in the period 2020-2100. We see that in all cases the area of the tropical ocean suitable for healthy coral growth expands, with the largest changes are associated with tropical addition (AOA_T). In some areas, such as the equatorial Pacific, the changes that have occurred since the preindustrial (1850) are also completely compensated, and in some cases leads to values that are higher than were experienced in the preindustrial period.

While the amount of alkalinity added in this study is small in comparison to other published studies, the challenge of achieving even this level of AOA should not be underestimated. Indeed, it is not clear whether such an effort is even feasible given the cost, logistical, political and engineering challenges of producing and distributing such large quantities of alkaline material (Renforth and Henderson, 2017). In the case of RCP8.5 it is unlikely that this level of AOA could be justified given our results. If emissions can be reduced along an RCP2.6 type trajectory this study suggests that AOA is much more effective and may provide a method to remove atmospheric CO_2 to complement mitigation, albeit with some side-effects, and an alternative to reliance on land based CDR.

In this work, and other published studies to date, we have not accounted for role of the mesoscale in AOA. In the real ocean (mesoscale) eddies are ubiquitous, and associated with strong convergent and divergent flows, and mixing that plays an important role in ocean transport (Zhang et al., 2014b). It is plausible that the mesoscale, and indeed fine scale circulation in the coastal environment e.g. (Mongin et al., 2016a;Mongin et al., 2016b) would modulate the response to AOA and therefore needs to be considered in future studies.

Furthermore, this is a single model study, and the results of this work need to be tested and compared in other models. The Carbon Dioxide Removal Model Intercomparison Project (CDR-MIP) was created to coordinate and advance the understanding of CDR in the earth system (Lenton et al., 2017). CDR-MIP brings together Earth System models of varying complexity in a series of coordinated multi-model experiments, one of which is a global AOA experiment (C4) (Keller et al., 2017). This will allow the response of the earth system to AOA to be further explored and quantified in a robust multi-model framework, and will

examine important further questions such as including cessation effects of alkalinity addition, and the long-term fate of additional alkalinity in the ocean. In parallel, more process and observational studies e.g. mesocosm experiments, are needed to better understand the implications of AOA.

5. Acknowledgments

D. P. Keller acknowledges funding received from the German Research Foundation's Priority Program 1689 "Climate Engineering" (project CDR-MIA; KE 2149/2-1). The authors declare that there are no conflicts of interest. The model code, simulations and scripts used in this study are available by contacting Andrew Lenton (andrew.lenton@csiro.au). We wish to also to thank Tom W. Trull for his helpful comments on this manuscript.

6. Biblography

Albright, R., Caldeira, L., Hosfelt, J., Kwiatkowski, L., Maclaren, J. K., Mason, B. M., Nebuchina, Y., Ninokawa, A., Pongratz, J., Ricke, K. L., Rivlin, T., Schneider, K., Sesboue, M., Shamberger, K., Silverman, J., Wolfe, K., Zhu, K., and Caldeira, K.: Reversal of ocean acidification enhances net coral reef calcification, Nature, 531, 362-+, 10.1038/nature17155, 2016.

Best, M. J., Abramowitz, G., Johnson, H. R., Pitman, A. J., Balsamo, G., Boone, A., Cuntz, M., Decharme, B., Dirmeyer, P. A., Dong, J., Ek, M., Guo, Z., Haverd, V., Van den Hurk, B. J. J., Nearing, G. S., Pak, B., Peters-Lidard, C., Santanello, J. A., Stevens, L., and Vuichard, N.: The Plumbing of Land Surface Models: Benchmarking Model Performance, J Hydrometeorol, 16, 1425-1442, 10.1175/JHM-D-14-0158.1, 2015.

Chavez, F. P., Ryan, J., Lluch-Cota, S. E., and Niquen, M.: From anchovies to sardines and back: Multidecadal change in the Pacific Ocean, Science, 299, 217-221, Doi 10.1126/Science.1075880, 2003.

Colbourn, G., Ridgwell, A., and Lenton, T. M.: The time scale of the silicate weathering negative feedback on atmospheric CO2, Global Biogeochemical Cycles, 29, 583-596, 10.1002/2014GB005054, 2015.

D'Olivo, J. P., and McCulloch, M. T.: Response of coral calcification and calcifying fluid composition to thermally induced bleaching stress, Scientific reports, 7, Artn 2207 10.1038/S41598-017-02306-X, 2017.

de Boyer Montegut, C., Madec, G., Fischer, A. S., Lazar, A., and Iudicone, D.: Mixed layer depth over the global ocean: An examination of profile data and a profile-based climatology, J Geophys Res-Oceans, 109, Artn C12003 10.1029/2004jc002378, 2004.

Doney, S. C., Ruckelshaus, M., Duffy, J. E., Barry, J. P., Chan, F., English, C. A., Galindo, H. M., Grebmeier, J. M., Hollowed, A. B., Knowlton, N., Polovina, J., Rabalais, N. N., Sydeman, W. J., and Talley, L. D.: Climate Change Impacts on Marine Ecosystems, Annu Rev Mar Sci, 4, 11-37, Doi 10.1146/Annurev-Marine-041911-111611, 2012.

Dore, J. E., Lukas, R., Sadler, D. W., Church, M. J., and Karl, D. M.: Physical and biogeochemical modulation of ocean acidification in the central North Pacific, P Natl Acad Sci USA, 106, 12235-12240, Doi 10.1073/Pnas.0906044106, 2009.

Duteil, O., Koeve, W., Oschlies, A., Aumont, O., Bianchi, D., Bopp, L., Galbraith, E., Matear, R., Moore, J. K., Sarmiento, J. L., and Segschneider, J.: Preformed and regenerated phosphate in ocean general circulation models: can right total concentrations be wrong?, Biogeosciences, 9, 1797-1807, 10.5194/bg-9-1797-2012, 2012.

Fabry, V. J., Seibel, B. A., Feely, R. A., and Orr, J. C.: Impacts of ocean acidification on marine fauna and ecosystem processes, Ices J Mar Sci, 65, 414-432, Doi 10.1093/Icesjms/Fsn048, 2008.

Feely, R. A., Doney, S. C., and Cooley, S. R.: Ocean Acidification: Present Conditions and Future Changes in a High-CO2 World, Oceanography, 22, 36-47, Doi 10.5670/Oceanog.2009.95, 2009.

Feng, E. Y., Keller, D. P., Koeve, W., and Oschlies, A.: Could artificial ocean alkalinization protect tropical coral ecosystems from ocean acidification?, Environ Res Lett, 11, Artn 074008, doi:10.1088/1748-9326/11/7/074008, 2016.

Frolicher, T. L., and Joos, F.: Reversible and irreversible impacts of greenhouse gas emissions in multi-century projections with the NCAR global coupled carbon cycle-climate model, Clim Dynam, 35, 1439-1459, Doi 10.1007/S00382-009-0727-0, 2010.

Fuss, S., Canadell, J. G., Peters, G. P., Tavoni, M., Andrew, R. M., Ciais, P., Jackson, R. B., Jones, C. D., Kraxner, F., Nakicenovic, N., Le Quere, C., Raupach, M. R., Sharifi, A., Smith,

P., and Yamagata, Y.: Commentary: Betting on Negative Emissions, Nat Clim Change, 4, 850-853, 2014.
Gasser, T., Guivarch, C., Tachiiri, K., Jones, C. D., and Ciais, P.: Negative emissions physically needed to keep global warming below 2 degrees C, Nat Commun, 6, Artn 7958 10.1038/Ncomms8958, 2015.
Gattuso, J.-P., Magnan, A., Billé, R., Cheung, W. W. L., Howes, E. L., Joos, F., Allemand, D., Bopp, L., Cooley, S. R., Eakin, C. M., Hoegh-Guldberg, O., Kelly, R. P., Pörtner, H.-O., Rogers, A. D., Baxter, J. M., Laffoley, D., Osborn, D., Rankovic, A., Rochette, J., Sumaila, U. R., Treyer, S., and Turley, C.: Contrasting futures for ocean and society from different anthropogenic CO2 emissions scenarios, Science, 349, 10.1126/science.aac4722, 2015.
Gonzalez, M. F., and Ilyina, T.: Impacts of artificial ocean alkalinization on the carbon cycle and climate in Earth system simulations, Geophys Res Lett, 43, 6493-6502, 10.1002/2016GL068576, 2016.
Groeskamp, S., Lenton, A., Matear, R., Sloyan, B. M., and Langlais, C.: Anthropogenic carbon in the oceanSurface to interior connections, Global Biogeochemical Cycles, 30, 1682-1698, 10.1002/2016GB005476, 2016.
Hauck, J., Kohler, P., Wolf-Gladrow, D., and Volker, C.: Iron fertilisation and century-scale effects of open ocean dissolution of olivine in a simulated CO2 removal experiment, Environ Res Lett, 11, Artn 024007, doi:10.1088/1748-9326/11/2/024007, 2016.
Heinze, C.: Simulating oceanic CaCO3 export production in the greenhouse, Geophys. Res. Let., 31, 2004.
Hoegh-Guldberg, O., Mumby, P. J., Hooten, A. J., Steneck, R. S., Greenfield, P., Gomez, E., Harvell, C. D., Sale, P. F., Edwards, A. J., Caldeira, K., Knowlton, N., Eakin, C. M., Iglesias-Prieto, R., Muthiga, N., Bradbury, R. H., Dubi, A., and Hatziolos, M. E.: Coral reefs under rapid climate change and ocean acidification, Science, 318, 1737-1742, 10.1126/science.1152509, 2007.
Hughes, T. P., Kerry, J. T., Alvarez-Noriega, M., Alvarez-Romero, J. G., Anderson, K. D., Baird, A. H., Babcock, R. C., Beger, M., Bellwood, D. R., Berkelmans, R., Bridge, T. C., Butler, I. R., Byrne, M., Cantin, N. E., Comeau, S., Connolly, S. R., Cumming, G. S., Dalton, S. J., Diaz-Pulido, G., Eakin, C. M., Figueira, W. F., Gilmour, J. P., Harrison, H. B., Heron, S. F., Hoey, A. S., Hobbs, J. P. A., Hoogenboom, M. O., Kennedy, E. V., Kuo, C. Y., Lough, J. M., Lowe, R. J., Liu, G., Cculloch, M. T. M., Malcolm, H. A., Mcwilliam, M. J., Pandolfi, J. M., Pears, R. J., Pratchett, M. S., Schoepf, V., Simpson, T., Skirving, W. J., Sommer, B., Torda, G., Wachenfeld, D. R., Willis, B. L., and Wilson, S. K.: Global warming and recurrent mass bleaching of corals, Nature, 543, 373-+, 10.1038/nature21707, 2017.
Iglesias-Rodriguez, M. D., Halloran, P. R., Rickaby, R. E. M., Hall, I. R., Colmenero-Hidalgo, E., Gittins, J. R., Green, D. R. H., Tyrrell, T., Gibbs, S. J., von Dassow, P., Rehm, E., Armbrust, E. V., and Boessenkool, K. P.: Phytoplankton calcification in a high-CO2 world, Science, 320, 336-340, Doi 10.1126/Science.1154122, 2008.
Ilyina, T., Wolf-Gladrow, D., Munhoven, G., and Heinze, C.: Assessing the potential of calcium-based artificial ocean alkalinization to mitigate rising atmospheric CO2 and ocean acidification, Geophys Res Lett, 40, 5909-5914, 10.1002/2013GL057981, 2013.
Jickells, T. D., An, Z. S., Andersen, K. K., Baker, A. R., Bergametti, G., Brooks, N., Cao, J. J., Boyd, P. W., Duce, R. A., Hunter, K. A., Kawahata, H., Kubilay, N., laRoche, J., Liss, P. S., Mahowald, N., Prospero, J. M., Ridgwell, A. J., Tegen, I., and Torres, R.: Global iron connections between desert dust, ocean biogeochemistry, and climate, Science, 308, 67-71, Doi 10.1126/Science.1105959, 2005.
Jones, C. D., Arora, V., Friedlingstein, P., Bopp, L., Brovkin, V., Dunne, J., Graven, H., Hoffman, F., Ilyina, T., John, J. G., Jung, M., Kawamiya, M., Koven, C., Pongratz, J., Raddatz, T., Randerson, J. T., and Zaehle, S.: C4MIP-The Coupled Climate-Carbon Cycle

Model Intercomparison Project: experimental protocol for CMIP6, Geosci Model Dev, 9, 2853-2880, 10.5194/gmd-9-2853-2016, 2016.
Keller, D. P., Feng, E. Y., and Oschlies, A.: Potential climate engineering effectiveness and side effects during a high carbon dioxide-emission scenario, Nat Commun, 5, Artn 3304 10.1038/Ncomms4304, 2014.
Keller, D. P., Lenton, A., Scott, V., Vaughan, N. E., Bauer, N., Ji, D., Jones, C., Kravitz, B., Muri, H., and Zickfeld, K.: The Carbon Dioxide Removal Model Intercomparison Project (CDR-MIP): Rationale and experimental design, Geoscientific Model Development Discussions, 2017.
Kheshgi, H. S.: Sequestering Atmospheric Carbon-Dioxide by Increasing Ocean Alkalinity, Energy, 20, 915-922, Doi 10.1016/0360-5442(95)00035-F, 1995.
Kohler, P., Abrams, J. F., Volker, C., Hauck, J., and Wolf-Gladrow, D. A.: Geoengineering impact of open ocean dissolution of olivine on atmospheric CO2, surface ocean pH and marine biology, Environ Res Lett, 8, doi:10.1088/1748-9326/8/1/014009, 2013.
Le Quéré, C., Moriarty, R., Andrew, R. M., Peters, G. P., Ciais, P., Friedlingstein, P., Jones, S. D., Sitch, S., Tans, P., Arneth, A., Boden, T. A., Bopp, L., Bozec, Y., Canadell, J. G., Chini, L. P., Chevallier, F., Cosca, C. E., Harris, I., Hoppema, M., Houghton, R. A., House, J. I., Jain, A. K., Johannessen, T., Kato, E., Keeling, R. F., Kitidis, V., Klein Goldewijk, K., Koven, C., Landa, C. S., Landschützer, P., Lenton, A., Lima, I. D., Marland, G., Mathis, J. T., Metzl, N., Nojiri, Y., Olsen, A., Ono, T., Peng, S., Peters, W., Pfeil, B., Poulter, B., Raupach, M. R., Regnier, P., Rödenbeck, C., Saito, S., Salisbury, J. E., Schuster, U., Schwinger, J., Séférian, R., Segschneider, J., Steinhoff, T., Stocker, B. D., Sutton, A. J., Takahashi, T., Tilbrook, B., van der Werf, G. R., Viovy, N., Wang, Y. P., Wanninkhof, R., Wiltshire, A., and Zeng, N.: Global carbon budget 2014, 7, 47-85, 2015.
Lenton, A., and Matear, R. J.: The role of the Southern Annular Mode (SAM) in Southern Ocean CO2 uptake, Global Biogeochemical Cycles, 21, doi: 10:1029/2006GB002714, 2007.
Lenton, A., Tilbrook, B., Matear, R. J., Sasse, T. P., and Nojiri, Y.: Historical reconstruction of ocean acidification in the Australian region, Biogeosciences, 13, 1753-1765, 10.5194/bg-13-1753-2016, 2016.
Lenton, A., Keller, D. P., and Pfister, P.: How Will Earth Respond to Plans for Carbon Dioxide Removal?, EOS, 98, 10.1029/2017EO068385, 2017.
Lovelock, J. E., and Rapley, C. G.: Ocean pipes could help the Earth to cure itself, Nature, 449, 403-403, 10.1038/449403a, 2007.
Mao, J., Phipps, S. J., Pitman, A. J., Wang, Y. P., Abramowitz, G., and Pak, B.: The CSIRO Mk3L climate system model v1.0 coupled to the CABLE land surface scheme v1.4b: evaluation of the control climatology, Geosci Model Dev, 4, 1115-1131, 10.5194/gmd-4-1115-2011, 2011.
Matear, R. J., and Hirst, A. C.: Long term changes in dissolved oxygen concentrations in the ocean caused by protracted global warming, Global Biogeochemical Cycles, 17, 1125, 2003.
Matear, R. J., and Lenton, A.: Quantifying the impact of ocean acidification on our future climate, Biogeosciences, 11, 3965-3983, Doi 10.5194/Bg-11-3965-2014, 2014.
Mathesius, S., Hofmann, M., Caldeira, K., and Schellnhuber, H. J.: Long-term response of oceans to CO2 removal from the atmosphere, Nat Clim Change, 5, 1107-+, 10.1038/NCLIMATE2729, 2015.
Mongin, M., Baird, M. E., Hadley, S., and Lenton, A.: Optimising reef-scale CO2 removal by seaweed to buffer ocean acidification, Environ Res Lett, 11, Artn 034023 10.1088/1748-9326/11/3/034023, 2016a.
Mongin, M., Baird, M. E., Tilbrook, B., Matear, R. J., Lenton, A., Herzfeld, M., Wild-Allen, K., Skerratt, J., Margvelashvili, N., Robson, B. J., Duarte, C. M., Gustafsson, M. S. M.,

807 Ralph, P. J., and Steven, A. D. L.: The exposure of the Great Barrier Reef to ocean
808 acidification, Nat Commun, 7, Artn 10732
809 10.1038/Ncomms10732, 2016b.
810 Montserrat, F., Renforth, P., Hartmann, J., Leermakers, M., Knops, P., and Meysman, F. J.
811 R.: Olivine Dissolution in Seawater: Implications for CO2 Sequestration through Enhanced
812 Weathering in Coastal Environments, Environmental science & technology, 51, 3960-3972,
813 10.1021/acs.est.605942, 2017.
814 Mucci, A.: The Solubility of Calcite and Aragonite in Seawater at Various Salinities,
815 Temperatures, and One Atmosphere Total Pressure, Am J Sci, 283, 780-799, 1983.
816 Munday, P. L., Donelson, J. M., Dixson, D. L., and Endo, G. G. K.: Effects of ocean
817 acidification on the early life history of a tropical marine fish, P Roy Soc B-Biol Sci, 276,
818 3275-3283, Doi 10.1098/Rspb.2009.0784, 2009.
819 Munday, P. L., Dixson, D. L., McCormick, M. I., Meekan, M., Ferrari, M. C. O., and
820 Chivers, D. P.: Replenishment of fish populations is threatened by ocean acidification, P Natl
821 Acad Sci USA, 107, 12930-12934, Doi 10.1073/Pnas.1004519107, 2010.
822 National Research Council: Climate Intervention: Carbon Dioxide and the Reliable
823 Sequestration of Carbon Washington D.C., US, 2015.
824 Orr, J. C., Fabry, V. J., Aumont, O., Bopp, L., Doney, S. C., Feely, R. A., Gnanadesikan, A.,
825 Gruber, N., Ishida, A., Joos, F., Key, R. M., Lindsay, K., Maier-Reimer, E., Matear, R.,
826 Monfray, P., Mouchet, A., Najjar, R. G., Plattner, G. K., Rodgers, K. B., Sabine, C. L.,
827 Sarmiento, J. L., Schlitzer, R., Slater, R. D., Totterdell, I. J., Weirig, M. F., Yamanaka, Y.,
828 and Yool, A.: Anthropogenic ocean acidification over the twenty-first century and its impact
829 on calcifying organisms, Nature, 437, 681-686, 2005.
830 Phipps, S. J., Rotstayn, L. D., Gordon, H. B., Roberts, J. L., Hirst, A. C., and Budd, W. F.:
831 The CSIRO Mk3L climate system model version 1.0-Part 2: Response to external forcings,
832 Geosci Model Dev, 5, 649-682, 10.5194/gmd-5-649-2012, 2012.
833 Ragueneau, O., Treguer, P., Leynaert, A., Anderson, R. F., Brzezinski, M. A., DeMaster, D.
834 J., Dugdale, R. C., Dymond, J., Fischer, G., Francois, R., Heinze, C., Maier-Reimer, E.,
835 Martin-Jezequel, V., Nelson, D. M., and Queguiner, B.: A review of the Si cycle in the
836 modem ocean: recent progress and missing gaps in the application of biogenic opal as a
837 paleoproductivity proxy, Global Planet Change, 26, 317-365, Doi 10.1016/S0921-
838 8181(00)00052-7, 2000.
839 Raven, J., Caldeira, K., Elderfield, H., Hoegh-Guldberg, O., Liss, P., and Riebesell, U.:
840 Ocean acidification due to increasing atmospheric carbon dioxide. The Royal Society, Policy
841 Document, London, UK, 2005.
842 Renforth, P., and Henderson, G.: Assessing ocean alkalinity for carbon sequestration, Review
843 in Geophysics, 55, 10.1002/2016RG000533, 2017.
844 Revelle, R., and Suess, H. E.: Carbon dioxide exchange between atmosphere and ocean and
845 the question of an increase of atmospheric CO2 during the past decades, Tellus, 9, 18-27,
846 1957.
847 Riebesell, U., Zondervan, I., Rost, B., Tortell, P. D., Zeebe, R. E., and Morel, F. M. M.:
848 Reduced calcification of marine plankton in response to increased atmospheric CO2, Nature,
849 407, 364-367, 2000.
850 Riebesell, U., Fabry, V. J., Hansson, L., and Gattuso, J.-P.: Guide to best practices for ocean
851 acidification research and data reporting, Publications Office of the European Union.,
852 Luxembourg, 260, 2010.
853 Rogelj, J., Meinshausen, M., and Knutti, R.: Global warming under old an new scenarios
854 using IPCC climate sensitivity range estimates, Nat Clim Change, 2, 248-253,
855 10.1038/NCLIMATE1385, 2012.

Rogelj, J., den Elzen, M., Hohne, N., Fransen, T., Fekete, H., Winkler, H., Chaeffer, R. S., Ha, F., Riahi, K., and Meinshausen, M.: Paris Agreement climate proposals need a boost to keep warming well below 2 degrees C, Nature, 534, 631-639, 10.1038/nature18307, 2016.

Sabine, C. L., Feely, R. A., Gruber, N., Bullister, J. L., Wanninkhof, R., Wong, C. S., Wallace, D. W. R., Tilbrook, B., Millero, F. J., Peng, T.-H., Kozyr, A., Ono, T., and Rios, A. F.: The Oceanic Sink for Anthropogenic CO_2, Science, 305, 367-371, 2004.

Scott, V., Haszeldine, R. S., Tett, S. F. B., and Oschlies, A.: Fossil fuels in a trillion tonne world, Nat Clim Change, 5, 419-423, 10.1038/NCLIMATE2578, 2015.

Seneviratne, S. I., Corti, T., Davin, E. L., Hirschi, M., Jaeger, E. B., Lehner, I., Orlowsky, B., and Teuling, A. J.: Investigating soil moisture-climate interactions in a changing climate: A review, Earth-Science Reviews, 99, 125-161, 10.1016/j.earscirev.2010.02.004, 2010.

Sigman, D. M., and Boyle, E. A.: Glacial/interglacial variations in atmospheric carbon dioxide, Nature, 407, 859-869, Doi 10.1038/35038000, 2000.

Smith, P., Davis, S. J., Creutzig, F., Fuss, S., Minx, J., Gabrielle, B., Kato, E., Jackson, R. B., Cowie, A., Kriegler, E., van Vuuren, D. P., Rogelj, J., Ciais, P., Milne, J., Canadell, J. G., McCollum, D., Peters, G., Andrew, R., Krey, V., Shrestha, G., Friedlingstein, P., Gasser, T., Grubler, A., Heidug, W. K., Jonas, M., Jones, C. D., Kraxner, F., Littleton, E., Lowe, J., Moreira, J. R., Nakicenovic, N., Obersteiner, M., Patwardhan, A., Rogner, M., Rubin, E., Sharifi, A., Torvanger, A., Yamagata, Y., Edmonds, J., and Cho, Y.: Biophysical and economic limits to negative CO2 emissions, Nat Clim Change, 6, 42-50, 10.1038/NCLIMATE2870, 2016.

Society, T. R.: Geoengineering the Climate System: Sceonce Goverence and Uncertainity, London, UK, 2009.

Taylor, K. E., Stouffer, R. J., and Meehl, G. A.: An Overview of Cmip5 and the Experiment Design, B Am Meteorol Soc, 93, 485-498, 10.1175/BAMS-D-11-00094.1, 2012.

Trull, T. W., Rintoul, S. R., Hadfield, M., and Abraham, E. R.: Circulation and seasonal evolution of polar waters south of Australia: Implications for iron fertilizations for the Southern Ocean, Deep-Sea Research II, 48, 2439-2466, 2001.

United Nations Framework on Climate Change: Adoption of the Paris Agreement, 21st Conference of the Parties. 2015.

Wang, Y. P., Law, R. M., and Pak, B.: A global model of carbon, nitrogen and phosphorus cycles for the terrestrial biosphere, Biogeosciences, 7, 2261-2282, 10.5194/bg-7-2261-2010, 2010.

Yamamoto, A., Kawamiya, M., Ishida, A., Yamanaka, Y., and Watanabe, S.: Impact of rapid sea-ice reduction in the Arctic Ocean on the rate of ocean acidification, Biogeosciences, 9, 2365-2375, 10.5194/bg-9-2365-2012, 2012.

Yamanaka, Y., and Tajika, E.: The role of vertical fluxes of particulate organic material and calcite in the oceanic carbon cycle: Studies using a ocean biogeochemical general; circulation model, Global Biogeochemical Cycles, 10, 361-382, 1996.

Yool, A., Popova, E. E., and Coward, A. C.: Future change in ocean productivity: Is the Arctic the new Atlantic?, J Geophys Res-Oceans, 120, 7771-7790, 10.1002/2015JC011167, 2015.

Zeebe, R. E.: History of Seawater Carbonate Chemistry, Atmospheric CO2, and Ocean Acidification, Annu Rev Earth Pl Sc, 40, 141-165, 10.1146/annurev-earth-042711-105521, 2012.

Zhang, Q., Wang, Y. P., Matear, R. J., Pitman, A. J., and Dai, Y. J.: Nitrogen and phosphorous limitations significantly reduce future allowable CO2 emissions, Geophys Res Lett, 41, 632-637, 10.1002/2013GL058352, 2014a.

Zhang, Z. G., Wang, W., and Qiu, B.: Oceanic mass transport by mesoscale eddies, Science, 345, 322-324, 10.1126/science.1252418, 2014b.

Earth Syst. Dynam. Discuss., https://doi.org/10.5194/esd-2017-92
Manuscript under review for journal Earth Syst. Dynam.
Discussion started: 1 November 2017

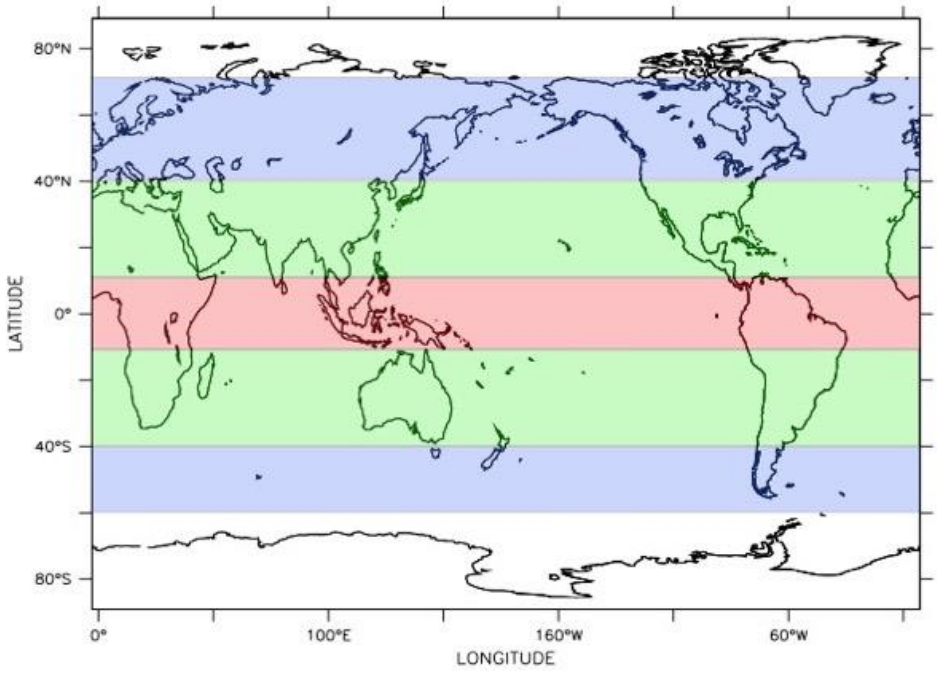

906

907 Figure 1 Ocean regions used for Alkalinity Injection in the period 2020-2100, the blue
908 denotes the subpolar regions (AOA_SP), the green regions represent the subtropical gyres
909 (AOA_ST), red the tropical ocean (AOA_T), and all colored regions combined the global
910 alkalinity injection (AOA_G). Note that the ocean regions not colored represent the seasonal
911 sea-ice, where no alkalinity was added in the simulation.

912

Earth Syst. Dynam. Discuss., https://doi.org/10.5194/esd-2017-92
Manuscript under review for journal Earth Syst. Dynam.
Discussion started: 1 November 2017

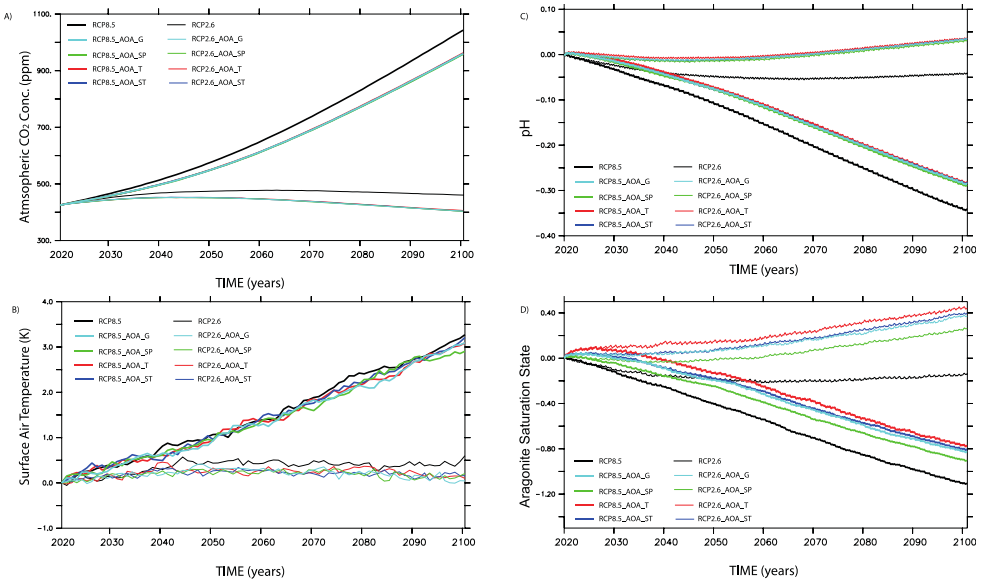

Figure 2 The global mean changes in: Atmospheric CO2 concentration (A), Surface Air Temperature (SAT; B), surface ocean pH (C) and Aragonite Saturation State (D) for high (RCP8.5) and low emissions (RCP2.6) with global and regional AOA in the period 2020-2100.

Earth Syst. Dynam. Discuss., https://doi.org/10.5194/esd-2017-92
Manuscript under review for journal Earth Syst. Dynam.
Discussion started: 1 November 2017

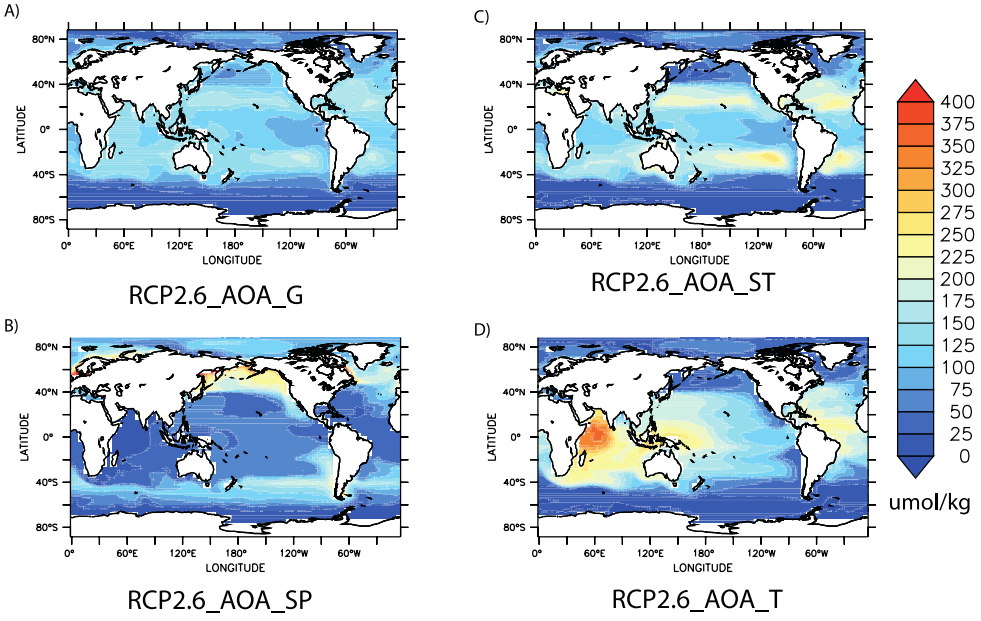

921
922

923

924 Figure 3 The spatial map of relative increase in surface alkalinity in 2090 (mean; 2081-2100)

925 associated with global and regional AOA under RCP2.6. Units are μmol/kg

926

Earth Syst. Dynam. Discuss., https://doi.org/10.5194/esd-2017-92
Manuscript under review for journal Earth Syst. Dynam.
Discussion started: 1 November 2017

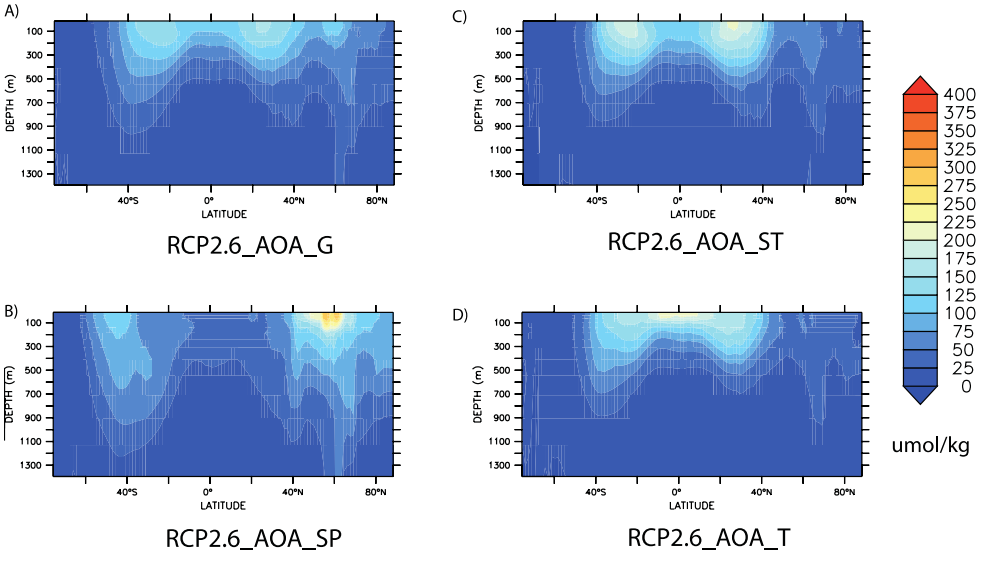

927
928
929 Figure 4 The zonal mean relative changes in alkalinity in the interior ocean associated with
930 global and regional AOA under RCP8.5 in 2090 (mean:2081-2100). Units are μmol/kg.
931

Earth Syst. Dynam. Discuss., https://doi.org/10.5194/esd-2017-92
Manuscript under review for journal Earth Syst. Dynam.
Discussion started: 1 November 2017

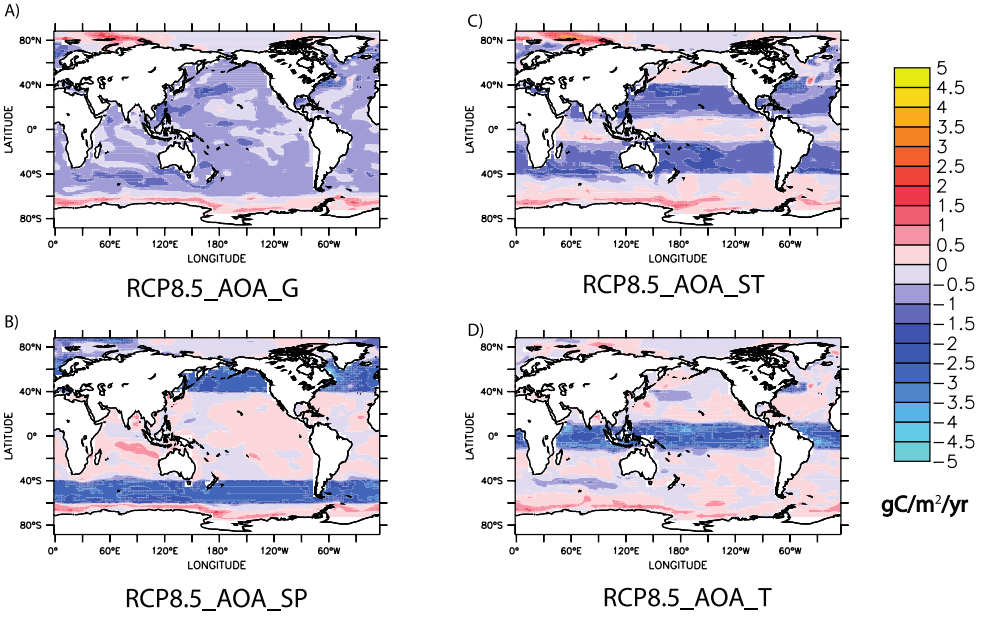

Figure 5 The spatial map of relative changes in ocean carbon uptake in 2090 (mean; 2081-2100) associated with global and regional AOA under RCP8.5. Units are gC/m^2/yr

Earth Syst. Dynam. Discuss., https://doi.org/10.5194/esd-2017-92
Manuscript under review for journal Earth Syst. Dynam.
Discussion started: 1 November 2017

937

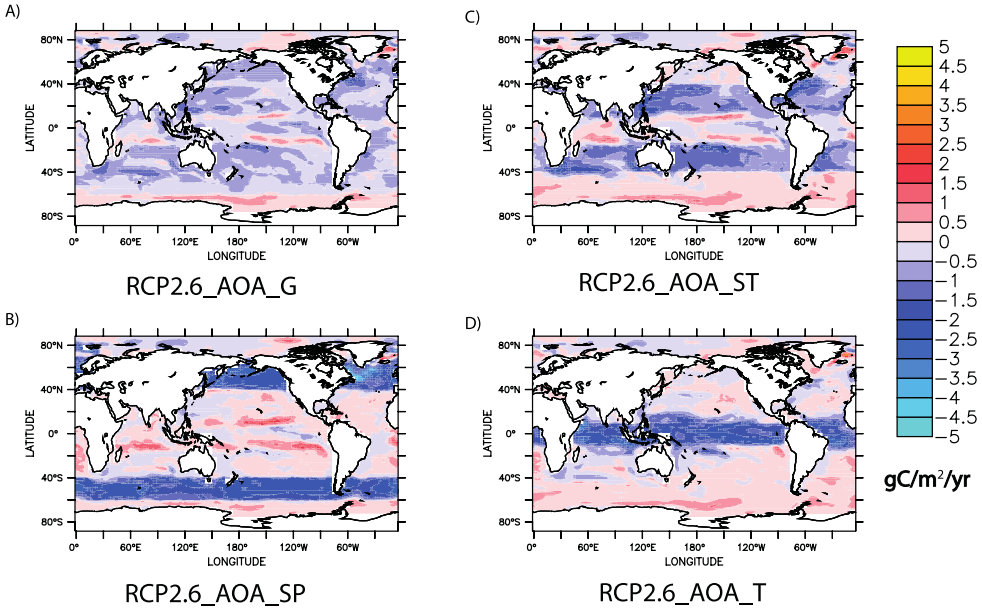

938

939 Figure 6 The spatial map of relative changes in ocean carbon uptake in 2090 (mean; 2081-
940 2100) associated with global and regional AOA under RCP2.6. Units are $gC/m^2/yr$

941

Earth Syst. Dynam. Discuss., https://doi.org/10.5194/esd-2017-92
Manuscript under review for journal Earth Syst. Dynam.
Discussion started: 1 November 2017

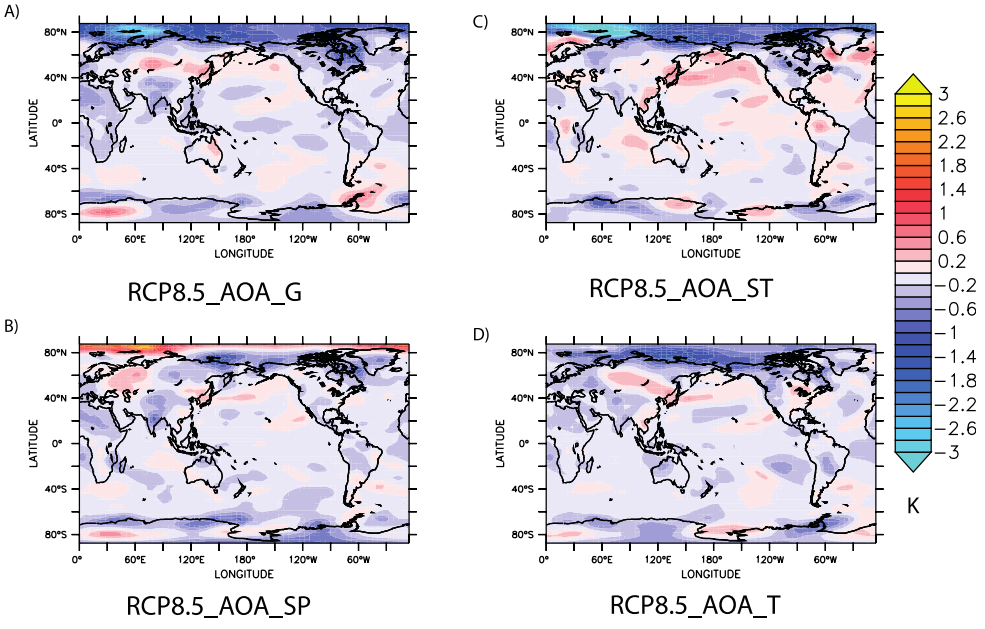

Figure 7 The spatial map of relative changes in surface air temperature 2090 (mean; 2081-2100) associated with global and regional AOA under RCP8.5. Units are K

Earth Syst. Dynam. Discuss., https://doi.org/10.5194/esd-2017-92
Manuscript under review for journal Earth Syst. Dynam.
Discussion started: 1 November 2017

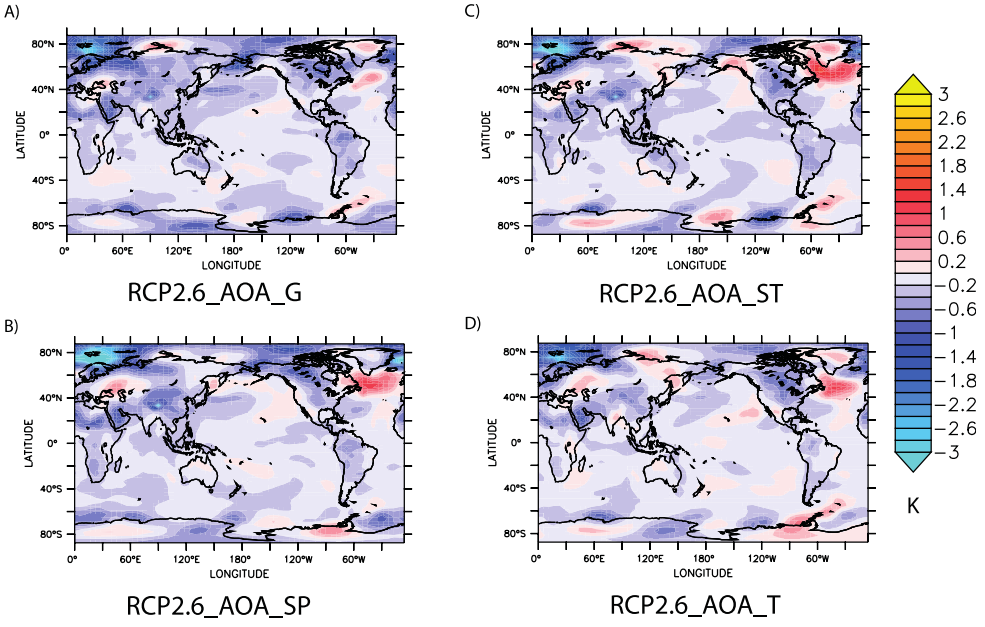

947
948
949 Figure 8 The spatial map of relative changes in surface air temperature 2090 (mean; 2081-
950 2100) associated with global and regional AOA under RCP2.6. Units are K
951

Earth Syst. Dynam. Discuss., https://doi.org/10.5194/esd-2017-92
Manuscript under review for journal Earth Syst. Dynam.
Discussion started: 1 November 2017

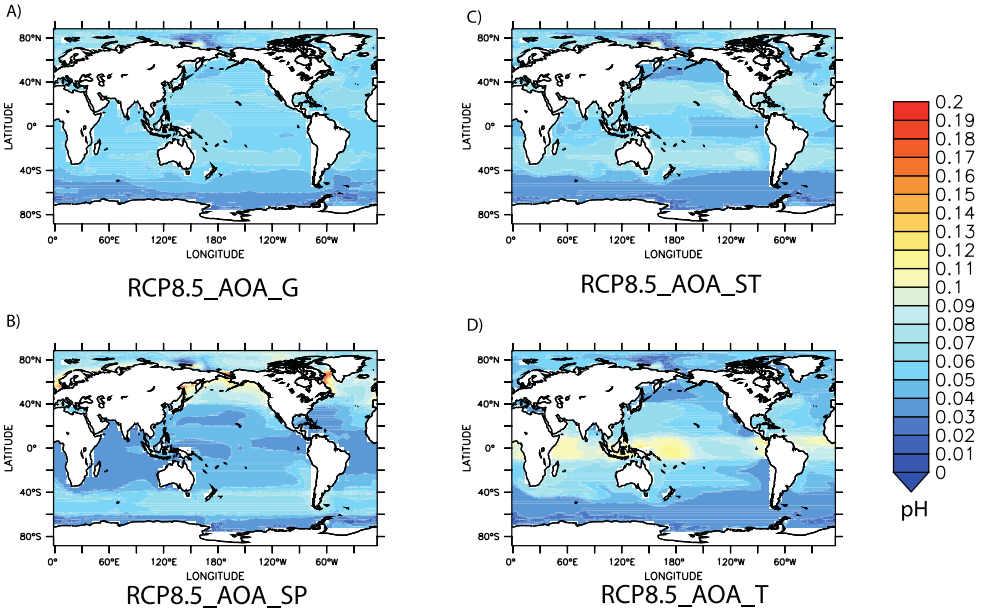

952
953
954 Figure 9 The spatial map of the relative changes in pH in 2090 (mean; 2081-2100) associated
955 with global and regional AOA under RCP8.5.
956

Earth Syst. Dynam. Discuss., https://doi.org/10.5194/esd-2017-92
Manuscript under review for journal Earth Syst. Dynam.
Discussion started: 1 November 2017

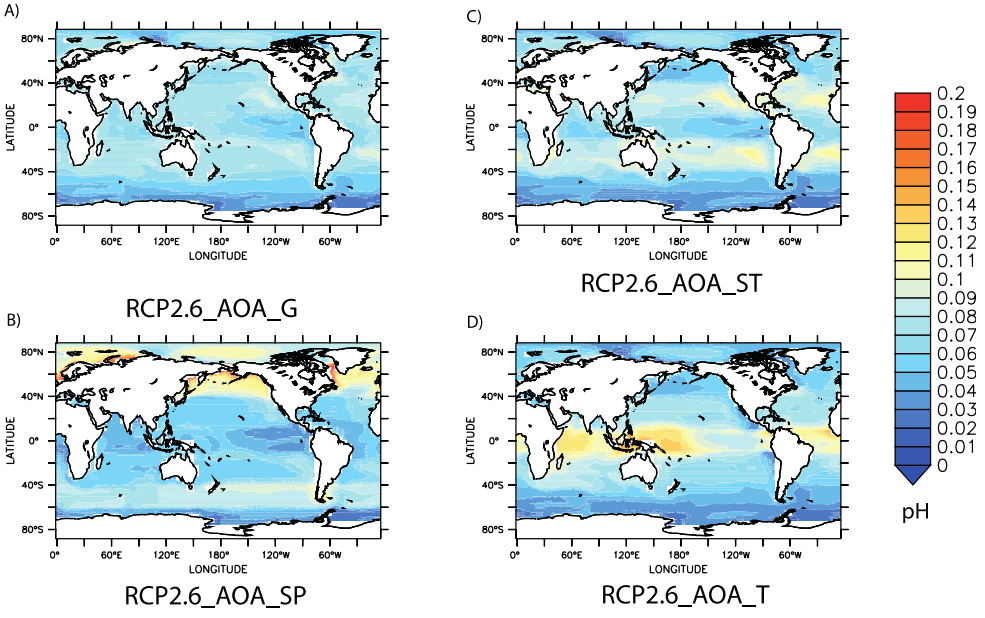

957
958
959 Figure 10 The spatial map of the relative changes in pH in 2090 (mean; 2081-2100)
960 associated with global and regional AOA under RCP2.6.
961

Earth Syst. Dynam. Discuss., https://doi.org/10.5194/esd-2017-92
Manuscript under review for journal Earth Syst. Dynam.
Discussion started: 1 November 2017

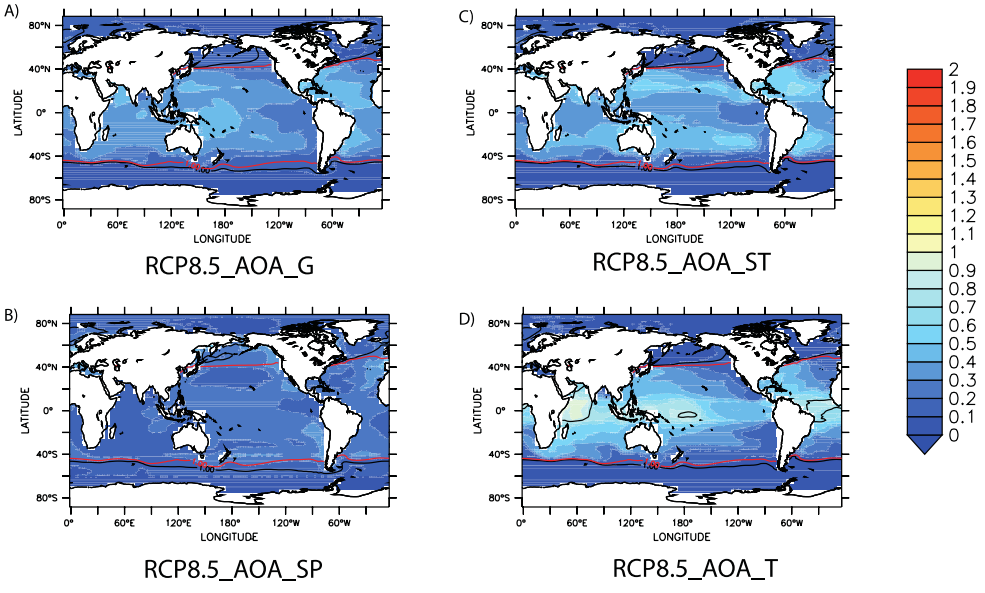

Figure 11 The spatial map of the relative differences in surface aragonite saturation state in 2090 (mean 2081-2100), associated with global and regional AOA under RCP8.5. Contoured on each map are the values of aragonite saturation state of 1 and 3, please see the text for more explanation. The red contours represent RCP8.5 and black AOA for each experiment

Earth Syst. Dynam. Discuss., https://doi.org/10.5194/esd-2017-92
Manuscript under review for journal Earth Syst. Dynam.
Discussion started: 1 November 2017

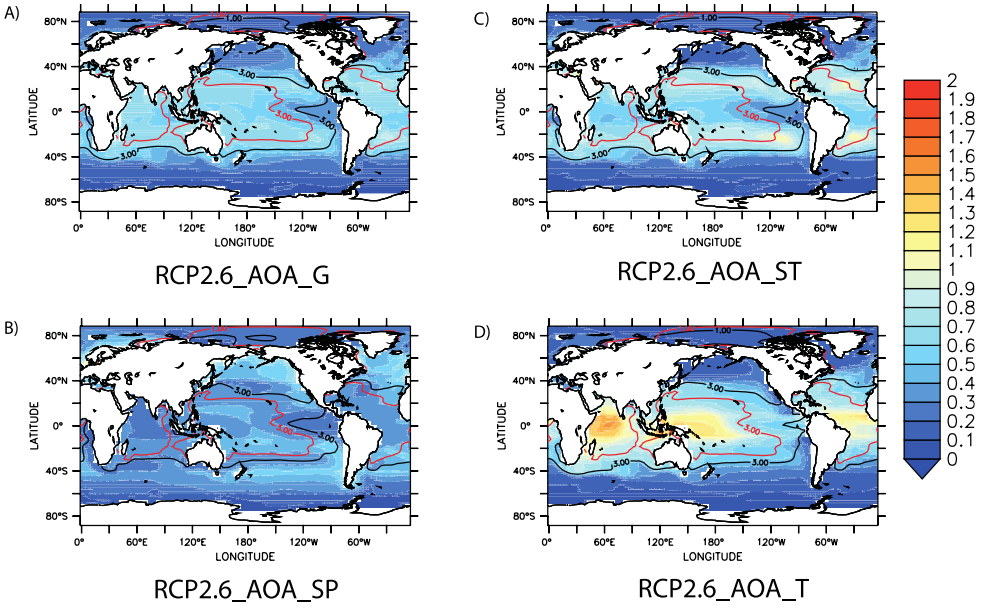

969
970
971 Figure 12 The spatial map of the relative differences in surface aragonite saturation state in
972 2090 (mean 2081-2100), associated with global and regional AOA under RCP2.6. Contoured
973 on each map are the values of aragonite saturation state of 1 and 3, please see the text for
974 more explanation. The red contours represent RCP2.6 and black AOA for each experiment
975

Earth Syst. Dynam. Discuss., https://doi.org/10.5194/esd-2017-92
Manuscript under review for journal Earth Syst. Dynam.
Discussion started: 1 November 2017

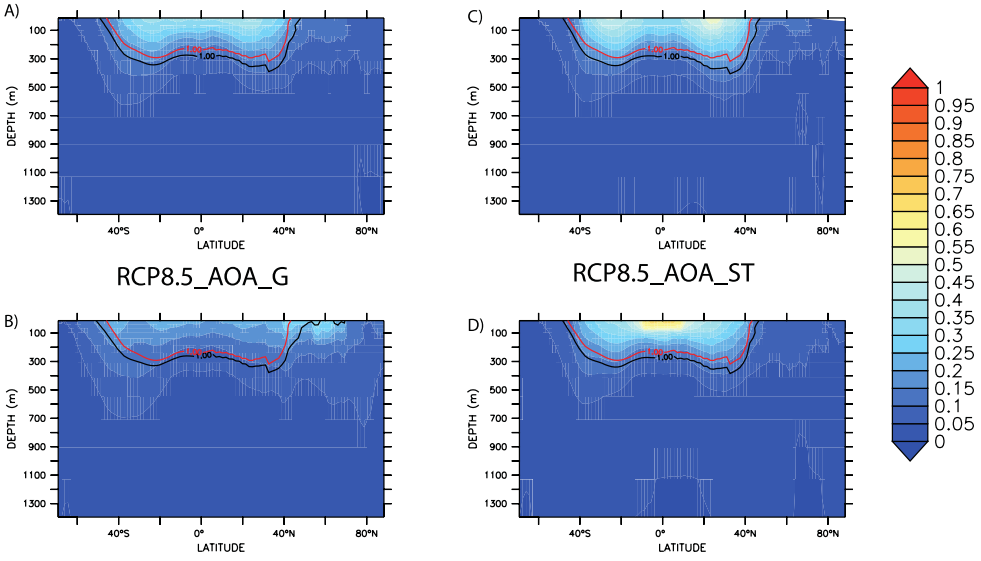

Figure 13 The relative zonal mean differences in aragonite saturation state in 2090 (mean 2081-2100), associated with global and regional AOA under RCP8.5. Contoured on each map are the values of aragonite saturation state of 1, please see the text for more explanation. The red contours represent RCP8.5 and black AOA for each experiment.

Earth Syst. Dynam. Discuss., https://doi.org/10.5194/esd-2017-92
Manuscript under review for journal Earth Syst. Dynam.
Discussion started: 1 November 2017

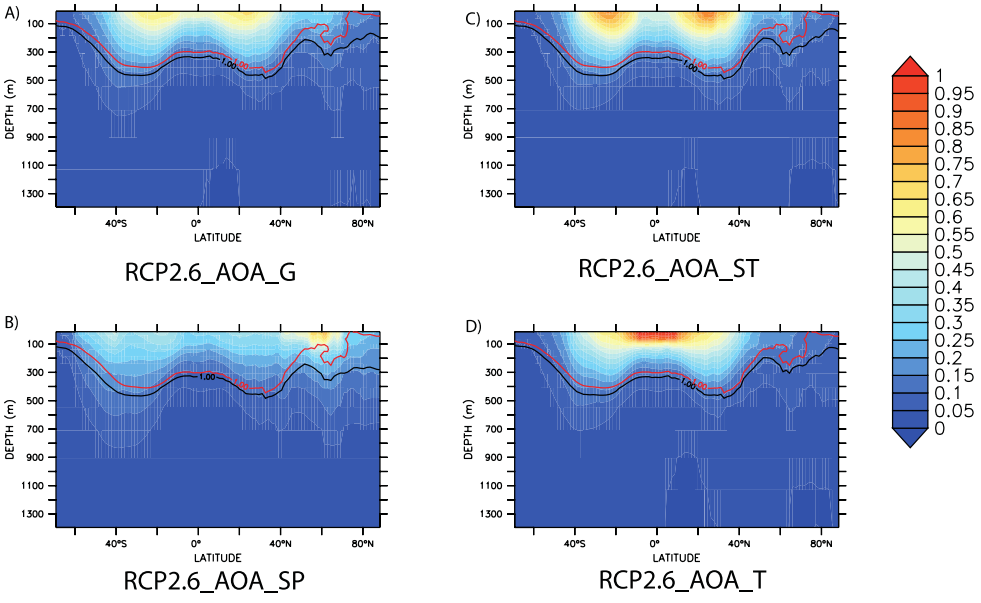

Figure 14 The relative zonal mean differences in aragonite saturation state in 2090 (mean 2081-2100), associated with global and regional AOA under RCP2.6. Contoured on each map are the values of aragonite saturation state of 1, please see the text for more explanation. The red contours represent RCP2.6 and black AOA for each experiment.